LEGO-BEL-AQ Deliverable D2.1.1

Low Earth and Geostationary Observations of BELgian Air Quality (LEGO-BEL-AQ):

Catalogue of high-resolution NO_2 maps: 1st version

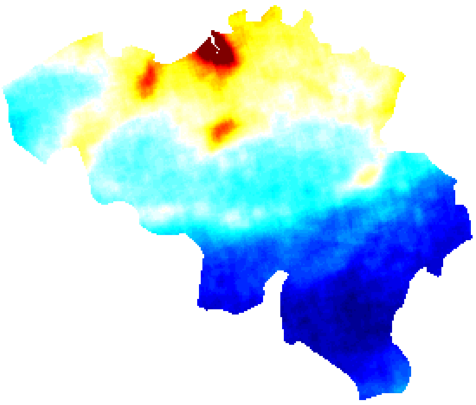

A BELSPO BRAIN-Be 2.0 project; Contract number: B2/191/P1/LEGO-BEL-AQ

Date: 10 March 2021

Beneficiary: BIRA-IASB

Nature: Other

Dissemination level: PU

Belgian Science Policy Office

belspo

BIRA•IASB

irCELine

Work Package	WP2 – APPLICATION OF THE WP1 TOOLBOX ON SENTINEL 5P NO_2 DATA OVER BELGIUM AND COMPARISON TO IN-SITU NETWORK DATA
Deliverable	D2.1.1
Title	Catalogue of high-resolution NO_2 maps, 1st version
Nature	Other
Dissemination	PU
Beneficiary	Royal Belgian Institute for Space Aeronomy (BIRA-IASB), Brussels, Belgium
Date	10 March 2021
Status	Version 1.1
Authors	Tijl Verhoelst, Steven Compernolle, Jean-Christopher Lambert
External Reviewer(s)	Laura Judd (NASA)
Contacts	tijl.verhoelst@aeronomie.be, j-c.lambert@aeronomie.be
URL	https://lego-bel-aq.aeronomie.be/

Cover image: 2019 average S5P-TROPOMI tropospheric NO_2 column over Belgium at a resolution of 1x1km2. Contains modified Copernicus data processed @ BIRA-IASB.

Table of Contents

Executive summary

One of the objectives of the LEGO-BEL-AQ project is the development and application of a toolset that allows the production of maps of atmospheric trace gases from low-earth-orbit (LEO) and geostationary (GEO) satellite observations, at a resolution above that of the individual level-2 measurements, essentially by trading temporal for spatial resolution. The aim behind these developments is to support air-quality related policy making at the local, regional, and national level in Belgium with fit-for-purpose observational data from the Copernicus atmospheric satellite constellation (S5P, S4, S5).

The current deliverable, D2.1.1, i.e. the first from WP2, deals with the first application of the first version of the toolset on S5P-TROPOMI tropospheric NO_2 columns to produce high-resolution maps of these columns over Belgium as a whole and several of its larger cities in particular. It describes the source data, the mapping procedure, the aggregation criteria, some example maps, the catalogue, and the data format and access. The example maps demonstrate that indeed, resolution can be gained by temporal aggregation and spatial oversampling, and that this increase in resolution is of interest as it allows us to distinguish and better localize several areas of persistent high NO_2 columns over Belgium. More specifically, we identify 3-monthly averages on a 1x1km^2 grid as a first “sweet spot” in the spatial/temporal resolution trade-off. This spatial sampling is significantly finer than that of individual pixels (3.5x5.5km^2 footprint at nadir and increasing with viewing angle) and the 3-month window ensures (1) sufficient observation density (needed to reduce grid-cell-to-grid-cell correlations) and (2) sufficient averaging out of features related to plume advection by winds. To avoid spurious features, some data filtering is needed before the mapping procedure, e.g. on L2 data quality indicators, cloud cover, and on solar zenith angle. Prospects for the further development of the catalogue are described as well.

1. Introduction

Air quality monitoring has hitherto been relying mostly on measurement networks of in-situ atmospheric composition, complemented with chemical transport modelling (CTM) to fill the gaps between measurements. The advent of hyperspectral satellite sounders observing at high spatial resolution (typically 5 x 5 km² on ground) has enabled global mapping of atmospheric pollutants at regional and even nearly local scales, but, only once per day and in cloud free weather, without access to the diurnal cycle of pollutants and of their emissions. In the next step, the international community has elaborated a strategy for integrated observation of air quality with a constellation of these satellites: the CEOS LEO+GEO AQ Constellation, gathering Low Earth Orbit instruments (LEO) with global mapping once per day, and Geostationary instruments (GEO) limited to a geographical area like Europe or North America but also with hourly sampling and thus access to the diurnal cycle. The European programme Copernicus contributes to this LEO+GEO AQ constellation with the Sentinel-5 Precursor (S5P) satellite since 2017 and the launch of several Sentinel-4 (GEO) and Sentinel-5 (LEO) after 2023.

One of the challenges to make these new data sets truly fit-for-purpose in the context of air quality policy making, is the need for even better horizontal resolution to map and monitor pollution on the scale of individual cities. This is particularly true for Belgium which is rather inhomogeneous both in population density and in air-quality related local policies (e.g. the Low Emission Zones established in several large Belgian cities). Work packages 1 and 2 of LEGO-BEL-AQ aim to contribute to this challenge by developing appropriate oversampling tools (WP1), and by applying these to Sentinel-5 precursor data over Belgium (WP2). In a first stage, several horizontal gridding scales and various temporal selection criteria are explored, both to maximize the achieved horizontal resolution and to uncover spatio-temporal patterns in the tropospheric NO_2 columns, as can be expected from variations in economic activity, heating, wind direction, etc. A catalogue of such maps is to be compiled for Belgium, the regions, and several major cities. The current deliverable concerns the 1st set of such maps. A following version of this deliverable, due end of 2021, will contain a further refinement and extension of the set of maps, including further advances in the mapping procedure.

In Sect. 2 we describe the level-2 (L2) data used to produce the maps, including some brief discussion of known data quality issues. Section 3 contains a high-level description of the mapping procedure, averaging the L2 data into a regularly gridded L3 product at a spatial sampling finer than the pixel size of the L2 data. The aggregation criteria for the averaging are detailed in Sect. 4. Some example high-resolutions maps with a very brief identification of observed features and potential NOx sources are presented in Sect. 5. The full catalogue, its data format, and file access are detailed in Sect. 6, and we conclude with some prospects in Sect. 7.

2. Observational data (S5P-TROPOMI level-2 data)

The retrieval of NO_2 (sub)columns from TROPOMI nadir radiance and solar irradiance spectra is a 3-step process relying on Differential Optical Absorption Spectroscopy and on a Chemical Transport Model (CTM) based stratosphere-troposphere separation. The TROPOMI NO_2 algorithm is an adaptation of the QA4ECV community retrieval approach (Boersma et al., 2018) and of the DOMINO/TEMIS algorithm (Boersma et al., 2007, 2011). Full details are available in van Geffen et al. (2020) and Eskes et al. (2020a, 2020b). The data used are the tropospheric NO_2 vertical columns from the OFFL (offline) operational L2 NO_2 product. For (near-)real time applications, there is also an NRTI product, but in the context of LEGO-BEL-AQ, the OFFL product is preferred as it uses meteorological data from an ECMWF forecast less far into the future (compared to the NRTI product) and the timeliness of about 10 days (as opposed to only a couple of hours for the NRTI product) is sufficient. If user needs collected during the project indicate that a timelier high-resolution NO_2 product would be of interest, the processing of NRTI files would be nearly identical and easily implemented. An overview of the different processor versions forming a continuous data set is provided in Table 1.

Table 1: Overview of the operational processor versions and their start and end dates.

Product	Processor	Version	Start orbit and date	End orbit and date
L2_NO2	NRTI	01.00.01	2955, 2018-05-09	3364, 2018-06-07
		01.00.02	3745, 2018-07-04	3946, 2018-07-18
		01.01.00	3947, 2018-07-18	5333, 2018-07-24
		01.02.00	5336, 2018-10-24	5929, 2018-12-05
		01.02.02	5931, 2018-12-05	7517, 2019-03-27
		01.03.00	7519, 2019-03-27	7999, 2019-03-30
		01.03.01	7999, 2019-03-30	9158, 2019-07-20
		01.03.02	9159, 2019-07-20	16258, 2020-12-02
		01.04.00	16259, 2020-12-02	current version
	OFFL	01.02.00	5236, 2018-10-17	5832, 2018-11-28
		01.02.02	5840, 2018-11-29	7424, 2019-03-20
		01.03.00	7425, 2019-03-20	7906, 2019-04-23
		01.03.01	7907, 2019-04-23	8814, 2019-06-26
		01.03.02	8815, 2019-06-26	16210, 2020-11-28
		01.04.00	16211, 2020-11-29	current version
	RPRO	01.02.02	2836, 2018-05-01	5235, 2018-10-17

Ground-based validation and intercomparison to other satellite data sets (in particular from the OMI instrument) suggests a low bias in TROPOMI tropospheric NO2, in particular for large columns, with an amplitude of roughly -30% w.r.t. the ground-based reference measurements from MAX-DOAS instruments (see Dimitropoulou et al., 2020, Verhoelst et al., 2021, and the S5P MPC-VDAF Quarterly Validation Reports available at https://mpc-vdaf.tropomi.eu/). Part of this low bias is expected to be removed with the latest processor upgrade, v1.4.0 (operational since early December 2020), which uses an updated cloud-retrieval scheme (FRESCO-WIDE) leading to lower cloud pressures and consequently larger tropospheric columns. First comparisons to OMI and ground-based reference data indeed indicate a reduced bias at polluted sites (Henk Eskes, private communication, and our own work for the MPC-VDAF). While the multiplicative nature of this bias implies that relative changes in tropospheric columns between different periods are mostly unaffected, the impact of this processor switch must be kept in mind. This will be resolved when the entire data set (from April 2019 to December 2020) is reprocessed with the latest processor version. This is planned/hoped to happen still in 2021.

3. Mapping procedure

The mapping procedure is described in full detail in deliverable D1.1.1 and its updates (Mapping toolbox and user manual). We provide here a summary of the methodology.

At the top level, the procedure is split into 3 steps:

1. Production of overpass L2 files for a region slightly larger than Belgium, to reduce the data volume to be treated in subsequent steps,
2. Filtering of the L2 data following (1) criteria on data quality and (2) aggregation desiderata,
3. Averaging of the filtered L2 data onto on L3 grid, taking into account the actual pixel/grid-cell overlap using area weights.

The area covered by the overpass files produced in the 1st step is shown in Figure 1. It contains Belgium and parts of the neighbouring countries, including major cities that –due to transport by winds- could contribute NOx over Belgium. If there is a user need for overpass data on other regions, e.g. for comparative purposes, these could be generated easily on demand.

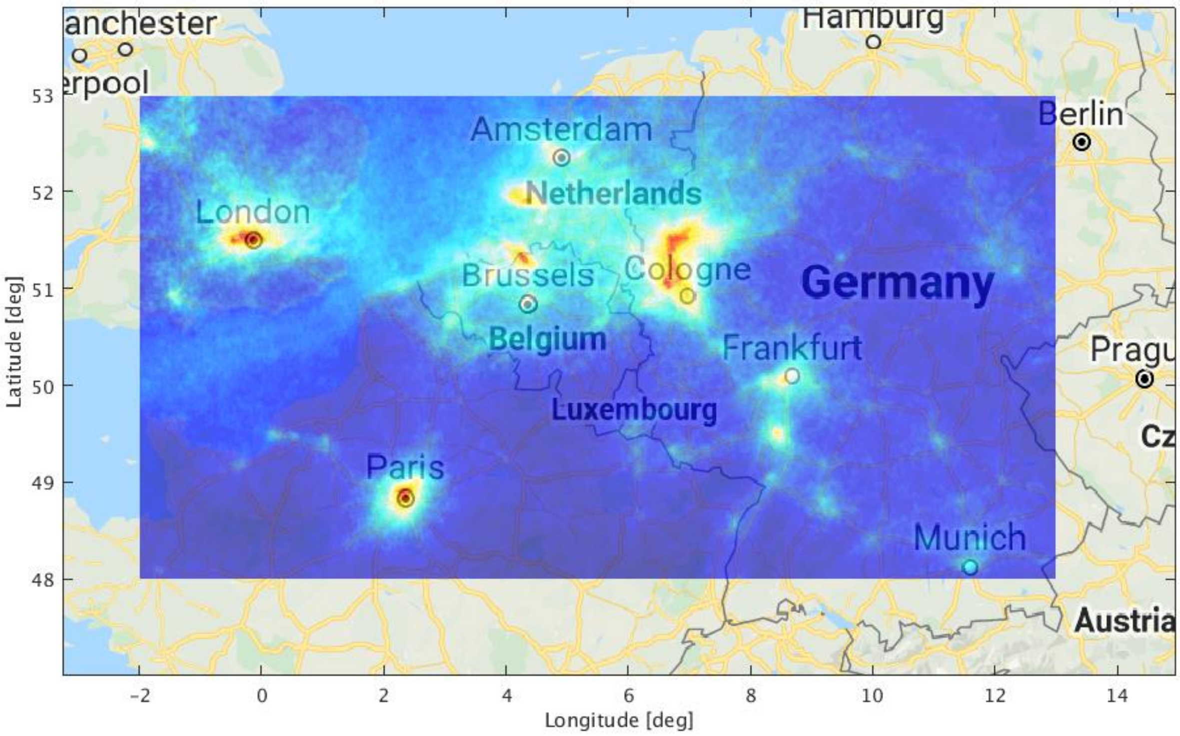

Figure 1: Area covered by the overpass files that are used in the gridding procedure, visualized by an overlay of gridded tropospheric NO_2 columns (3 months of summertime 2020 data on a 1x1km^2 grid).

The filtering is described in more detail in Section 4.

For the averaging onto the L3 grid (i.e. a regular latitude-longitude grid), we use the bin_spatial module of the HARP toolbox (https://atmospherictoolbox.org/harp/ and http://stcorp.github.io/harp/doc/html/operations.html). This routine calculates the area overlap between each intersecting L2 pixel and target L3 grid cell, in 2-D geometry (an acceptable approximation given the small pixels and grid cells targeted here, both having typical sizes of a few km). This area overlap is used as a weight in the averaging for a given grid cell. Mathematically:

$$VCD_{L3,j} = {\sum_i w_i VCD_{L2,i}}\Big/{\sum_i w_i}$$

where *i* runs over all L2 pixels intersecting the *j*-th L3 grid cell within the temporal averaging window, and w_i is calculated as:

$$w_i = {Area_{L2,i \cap L3,j}}\Big/{Area_{L3,j}}$$

A L2 pixel covering the entire L3 grid cell will thus have $w_i = 1$. The sum of the weights, i.e. $\sum_i w_i$, is available in the output files in order to have some quantitative information on the density of the data behind the L3 product. If an L3 grid cell was not covered entirely by L2 pixels, it will have a total weight below 1. If it was covered multiple times (even if only fractionally per L2 pixel), the total weight will exceed 1. We can thus consider this total weight a proxy for the total number of times the entire grid cell was observed. In many of the graphs in this document, the median total weight (indicated as median #obs/cell) over all the grid cells in the map is provided in the lower left corner.

An essential aim of the project being to trade temporal resolution for spatial resolution, the L3 grid cell size will be chosen smaller than the nominal L2 pixel size. Temporal averaging windows must be chosen large enough to ensure $\sum_i w_i \gg 1$ for each grid cell, because only then will we see a reduction in correlations between neighbouring grid cells due to contributions from the same L2 pixels. Indeed, as the orbit repeat cycle of S5p is 227 orbits, L2 pixels will have slightly different locations for each of 15 consecutive days.

The potential gains in spatial resolution are illustrated in Figure 2, which contains a comparison between a single orbit overpass and a 3-month gridded and oversampled average. While the true resolution of the oversampled image is probably not as high as the $1x1km^2$ sampling, the observed structures suggest a resolution well above that of a single S5p-TROPOMI overpass.

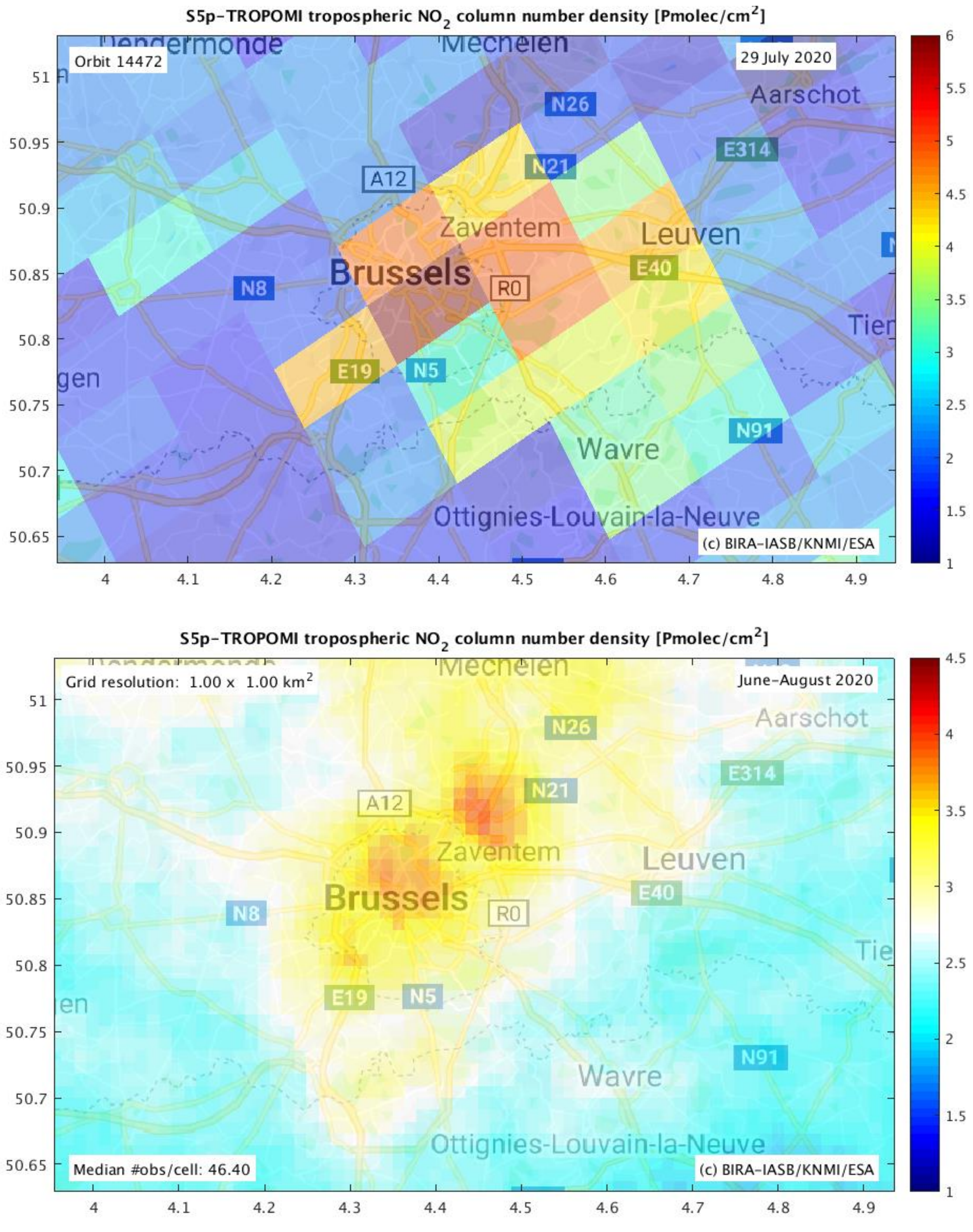

Figure 2: Comparison between tropospheric NO_2 columns measured in a single orbit overpassing Brussels, with pixel sizes of at best 5.5x3.5km^2 (upper panel), and the gridded and oversampled 3-month average for June-August 2020 at a 1x1km^2 grid resolution (lower panel). The area covered is identical in both panels.

4. Aggregation criteria

Several aggregation criteria can be considered, of both inclusive (e.g. temporal window) and exclusive (e.g. a quality filter) nature. Those explored for the production of the first set of maps are the following:

- Spatial averaging grid
- Temporal averaging window
- Temporal sampling frequency
- Solar zenith angle limits
- Wind speed limit
- Measurement quality (qa_value)

Many more can be of interest, such as week day versus week-end, but these will be explored in an update of the current deliverable (due M24, i.e. end of 2021). The choices made for each of these criteria for the first set of maps are summarized in Table 2, and we discuss below the motivation for each of them.

Table 2: Overview of the aggregation criteria used to produce the first set of LEGO-BEL-AQ maps.

Parameter	Value	Comments
Spatial averaging grid	1x1km^2	Technically: 0.0090 x 0.0143 deg^2
Temporal averaging window	91 days	Approx. 3 months
Temporal sampling frequency	15 days	Start date: 1 May 2019
Solar zenith angle limits	<75°	To avoid inclusion of early-morning or late-afternoon overpasses at low sun.
Wind speed limit	Not applied	Wind data not yet available for data pre March 2020. Averages over multiple months not highly affected.
qa_value	>0.75	Default recommendation for S5P tropospheric NO_2 columns.

Spatial Averaging grid

The spatial averaging grid should be sufficiently fine to resolve the point spread function (PSF) of the aggregated data, or, in other words, it should not limit the gain in actual resolving power by the data aggregation. Neither should it be taken too fine as this would result in only a few measurements per grid cell and consequently significant noise due to large sampling errors. As a first guestimate of an appropriate grid cell size, we use approx. 1x1km^2. As the aggregation actually occurs in lat-lon space, the true grid cell size used is 0.009x0.0143deg^2, which equals 1x1km^2 at a latitude of 51°N.

Temporal averaging window

At a given targeted horizontal gridding, the width of the temporal averaging window governs the compromise between temporal resolution and underlying data density. While daily maps, based on only one or a couple of overpasses, can reveal very specific events (e.g. heavy pollution transported by strong winds), they will in most cases suffer large gaps due to clouds or other retrieval-complicating conditions. Moreover, at these temporal scales, the observed NO2 field is heavily affected by the meteorological conditions and as such not necessarily representative for the "normal" regime. In view of the objectives of the project, interesting temporal windows are rather in the weeks-months range. While gap-free NO_2 maps of Belgium can be obtained in summertime from as little as 1 week of data, heavy cloud cover in winter translates into minimum temporal averaging windows of at least a month. This is illustrated in Figure 4.

As the focus of the project is on long-term evolution, we have chosen seasonal (91-day) averages. This ensures complete coverage with strong data density, even in winter time.

Temporal sampling frequency

To ensure a smooth, continuous sampling of the temporal evolution, the sampling needs to be significantly higher than the averaging window. We opted for a sampling rate of one seasonal average every 15 days.

Solar zenith angle limits

While the nominal overpass time of S5p is 1:30pm (local solar time for the sub-satellite point), mid- and high-latitude regions may benefit from multiple overpasses per day. For Belgium, the main overpass occurs around 12:30am UTC, and additional overpasses occasionally occur one orbit earlier (11am UTC) and one orbit later (2pm UTC). As the (relative) concentrations of NOx depend strongly on the insolation, mixing overpasses of different local solar times may lead to artificial structures (e.g. striping). This effect is most pronounced when including low-sun observations obtained close to twilight. For this reason, we remove observations with SZA>75°. In particular in winter this implies some data loss, as shown in Figure 3.

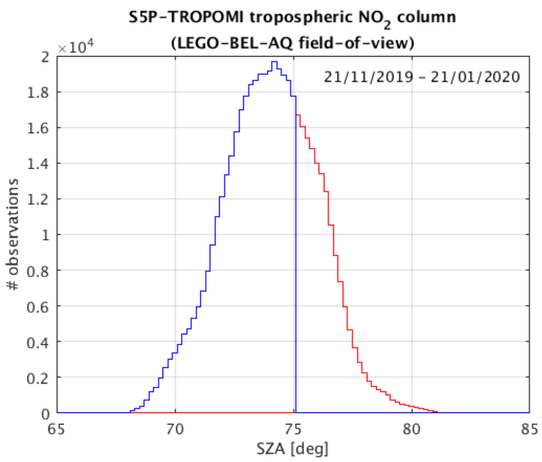

Figure 3: Histogram of the Solar Zenith Angle of the S5P-TROPOMI tropospheric NO2 column observations over Belgium during winter 2019-2020, with an indication of the cut-off at 75° used here to avoid artificial patterns in the maps due to the mixing of data corresponding to very different photochemical regimes. This being winter, it represents the worst case scenario (largest data loss due to the filter).

Wind speed limit

In case of significant boundary layer winds, advection of locally emitted NOx is clearly observable as plumes originating in strong emission sources. In a densely populated area such as Belgium, this leads to a highly structured NO2 map with potentially overlapping plumes. A couple of days with strong winds from a single prevailing direction (often from the South-West in Belgium) may therefor impact strongly a weekly or monthly NO2 map. Depending on the targeted use of the map, it may be advisable to filter out such days with strong winds. L2 data files produced since March 2020 contain the necessary *u* and *v* surface wind components. For earlier dates, wind info will be included in the L2 files when a full reprocessing is performed (targeted to happen still within 2021). Wind info can of course also be obtained directly from meteorological reanalyses, such as ECMWF's ERA-5.

We found that for averages over multiple months, the variability in wind direction ensures that emission sources still pop up, as these "stack up" consistently, while the advected plumes are diluted over the various directions. Consequently, the first set of maps presented here does not contain any filtering on wind speed. Future versions of the catalogue, containing shorter temporal averages, will make use of wind-speed filtering and will include wind roses in the graphical output to indicate the strength and direction of the prevailing wind.

qa_value

As a filter on L2 data quality, we use the default recommendation for the tropospheric columns of qa_value>0.75 (see the applicable Product Readme File at http://www.tropomi.eu/documents/prf). This ensures reliable retrievals under clear or only slightly cloudy conditions. This renders obsolete a separate filter on cloudiness.

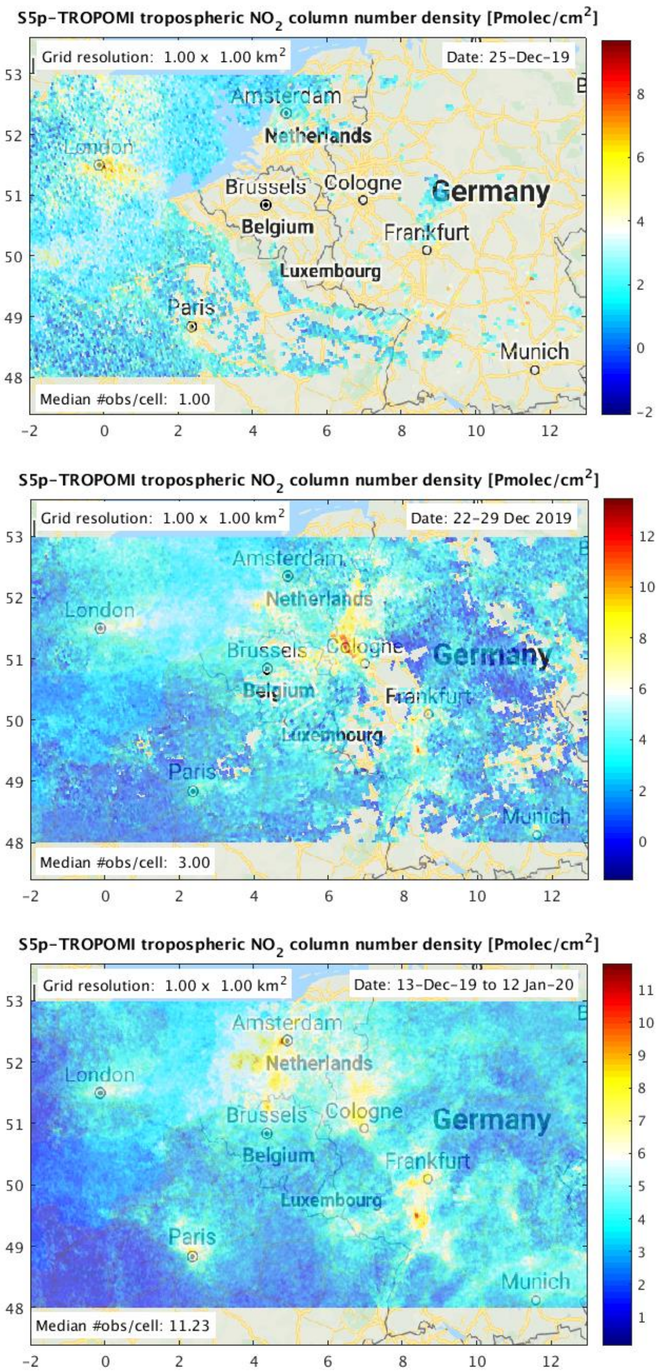

Figure 4: Illustration of the impact of different temporal averaging windows on the gaps due to cloud cover in local winter (these examples are centred on Christmas day 2019), and on the median number of observations per grid cell. *Top panel*: just one day and large gaps, *middle panel*: one week with just a few gaps remaining but low data density overall, and *lower panel*: complete coverage with a reasonable amount of measurements for each grid cell. For the 91-day averages used in the current version of the full catalogue, the median number of measurements per grid cell increases further to approximately 30 (in winter).

5. Example maps

This section contains several example maps of gridded oversampled S5p-TROPOMI tropospheric NO_2 columns with a brief description of observed features. The specifications of the full catalogue and instructions for file access are presented in the next section (Sect. 6).

5.1. Belgium

In Figure 5, we show the gridded data over all of Belgium for the 3-month period June-August 2020. This period corresponds to the period in the COVID-19 pandemic between the 1st and 2nd waves (in Belgium), with rather relaxed constraints on mobility and economic activities. Short NOx lifetimes in summer (due to strong insolation) reduce the impact of pollutant transport by winds.

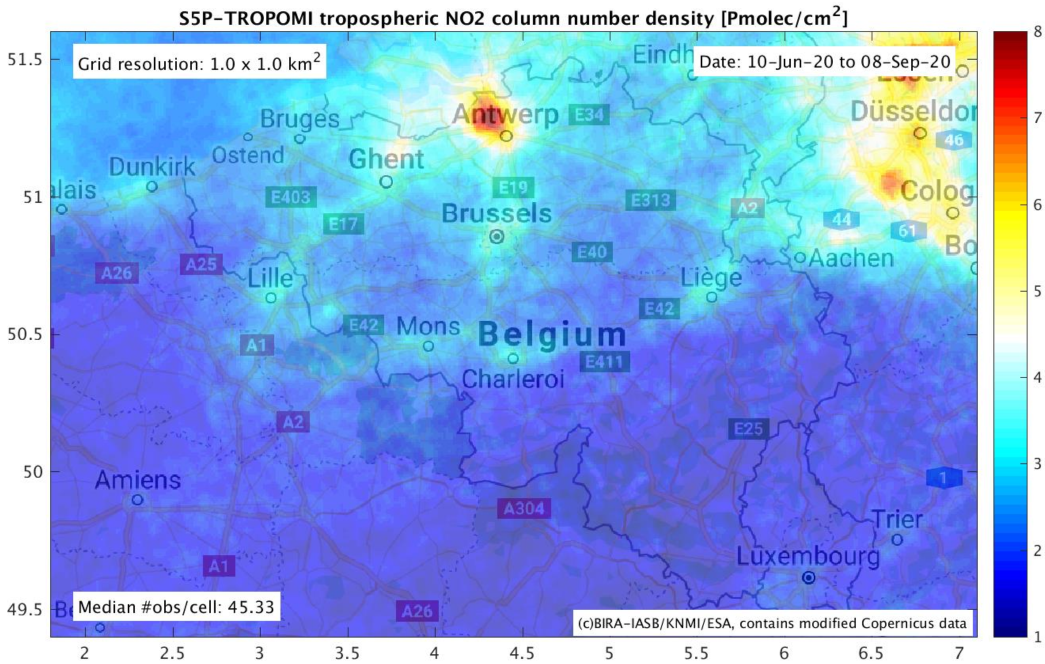

Figure 5: Map of S5p-TROPOMI tropospheric NO_2 column data over Belgium, OFFL processor versions v1.3.x, filtered on qa_value>0.75, and gridded to a 1x1km^2 resolution using data from June to August 2020.

Clear features are the hot spots over the harbor of Antwerp and in the east of Germany. Also showing elevated NO_2 levels are Ghent, Brussels, Charleroi and Liège. NO_2 levels are clearly much lower in the Ardennes. In this 3-month summer average, no clear transport features are evident. In view of the dominating Westerlies over Belgium, these would typically be oriented (South-)West to (North-)East. Detailed maps for several cities are discussed in the following sections.

5.2. Antwerp

In Figure 6, we show the gridded tropospheric NO_2 column data over the city of Antwerp and its surroundings for the period June-August 2020. During this period, peak values are observed mostly above the harbour. The tropospheric columns above the city centre, in particular the Southern parts, are substantially lower.

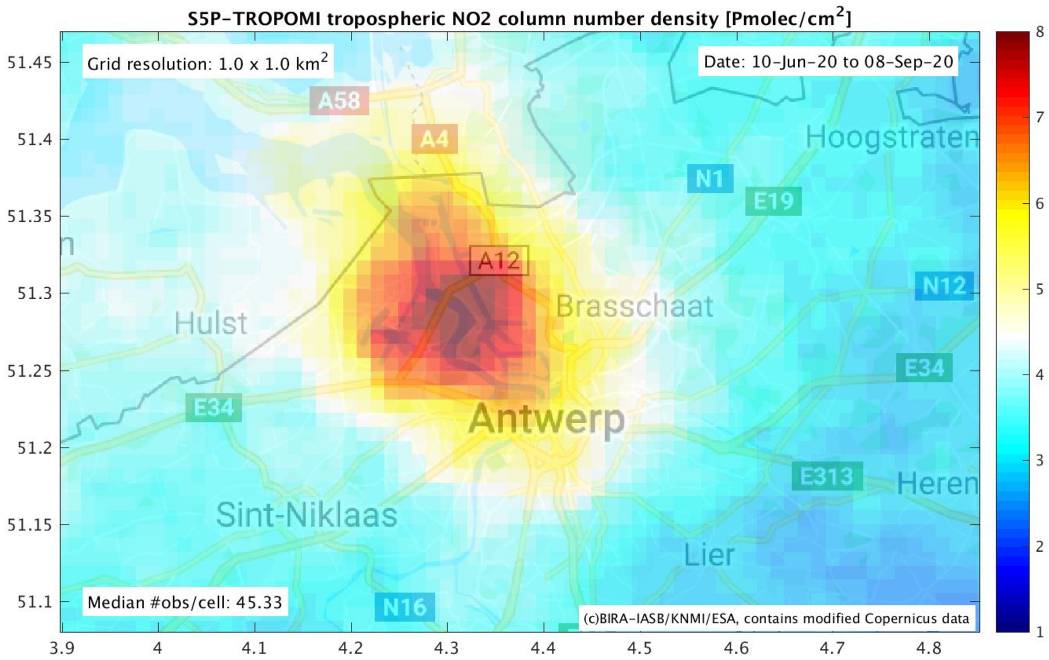

Figure 6: Map of S5p-TROPOMI tropospheric NO_2 column data over Antwerp, OFFL processor versions v1.3.x, filtered on qa_value>0.75, and gridded to a 1x1km^2 resolution using data from June to August 2020.

5.3. Brussels

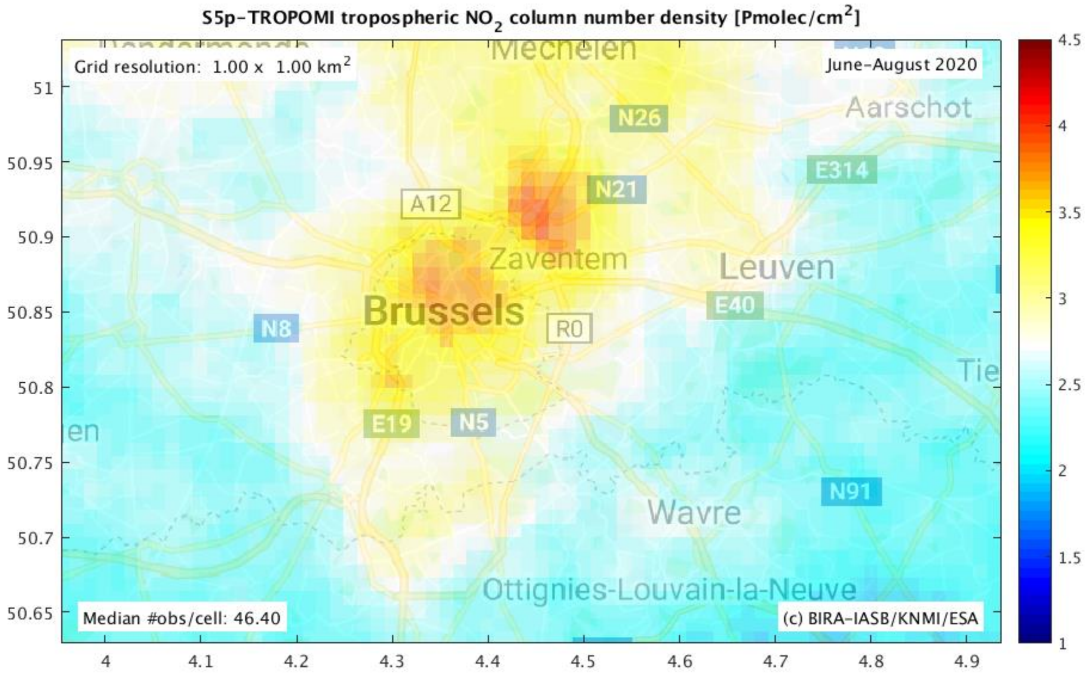

Figure 7: Map of S5p-TROPOMI tropospheric NO_2 column data over Brussels and it's surroundings, OFFL processor versions v1.3.x, filtered on qa_value>0.75, and gridded to a 1x1km^2 resolution using data from June to August 2020.

In Figure 7, we show the gridded data over the city of Brussels and its surroundings for the period June-August 2020. During this period, we can distinguish separate pollution highs over Brussels itself (inside the R0 ringroad), and the communes to the North-East: Zaventem, which hosts the national airport, and Machelen and Vilvoorde which are economic hot spots (both logistics and offices). Remarkable are the relatively low NO_2 levels along the R0 ringroad in between Brussels and Zaventem, known for it's structural traffic jams. For comparison, summer 2019 data for the same region are shown in Figure 8, using the same color scale. NO2 levels were substantially higher (up to 50%) at that time, also in the "pseudo-rural" region South-East and West of Brussels. Also observed are increased levels along the highways to the North (A12, towards Antwerp), and to the East (E40, towards Leuven). As meteorology is not expected to be very different over these 3-month averages for 2019 and 2020, these results could be related to reduced activity and mobility because of the COVID-19 pandemic, even if restrictions on both were relatively relaxed at this time.

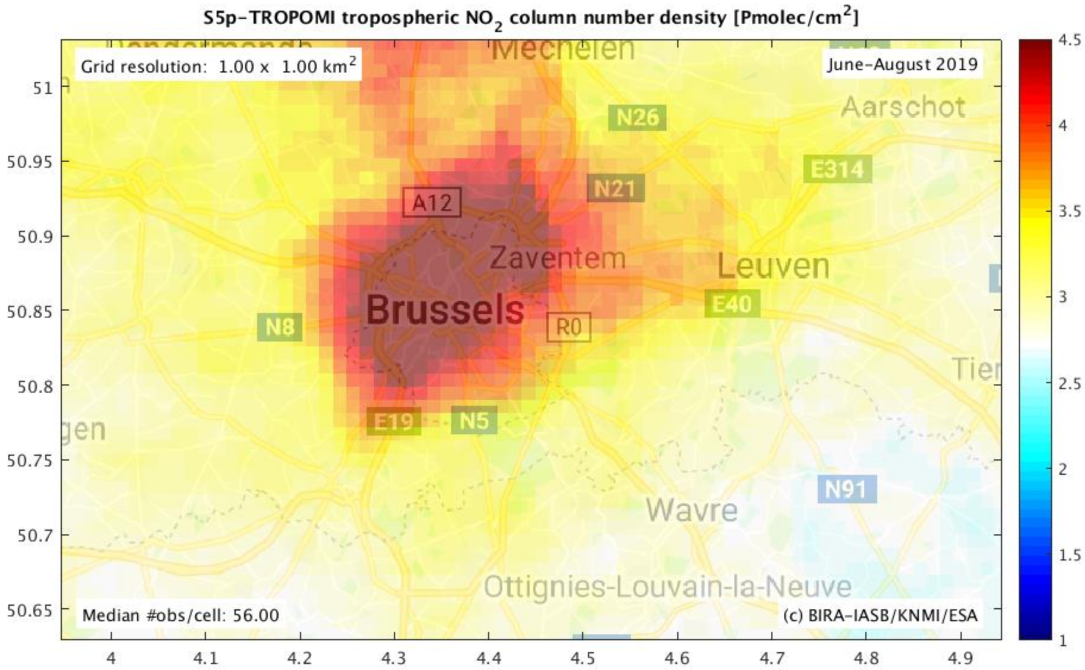

Figure 8: Similar to Figure 7 but using data from June to August 2019. For ease of comparison, the color scale is identical to that of Figure 7. This results in saturated values above the city centre and above Zaventem, Machelen and Vilvoorde. Even at wider color scale (not shown) Brussels and Zaventem are no longer distinguishable, probably due to a larger traffic volume on the Brussels ring road running in between.

5.4. Mons to Charleroi

In Figure 9, we show the gridded data over the region from Mons to Charlerio in Hainaut, revealing moderate hot spots above Mons, Charlerio and at the Northern edge of La Louvière, an industrial town hosting a site of NLMK (Novolipetsk) steelworks. The hot spot furthest to the East is Sambreville, which hosts several glassworks along the river Sambre.

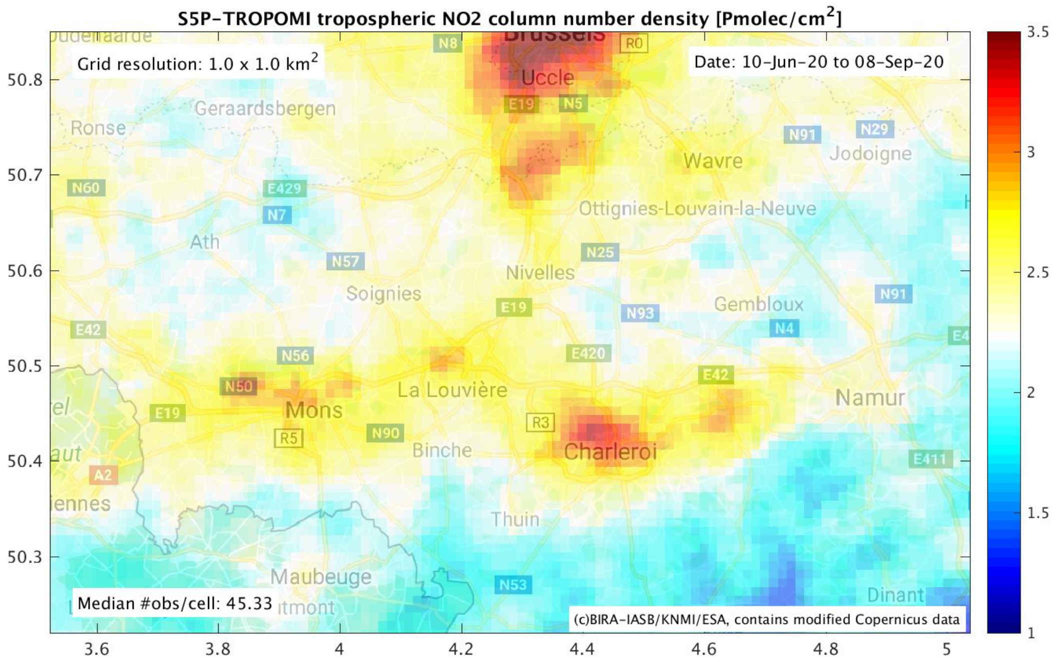

Figure 9: Map of S5p-TROPOMI tropospheric NO_2 column data over Mons and Charleroi, OFFL processor versions v1.3.x, filtered on qa_value>0.75, and gridded to a 1x1km^2 resolution using data from June to August 2020.

5.5. Ghent

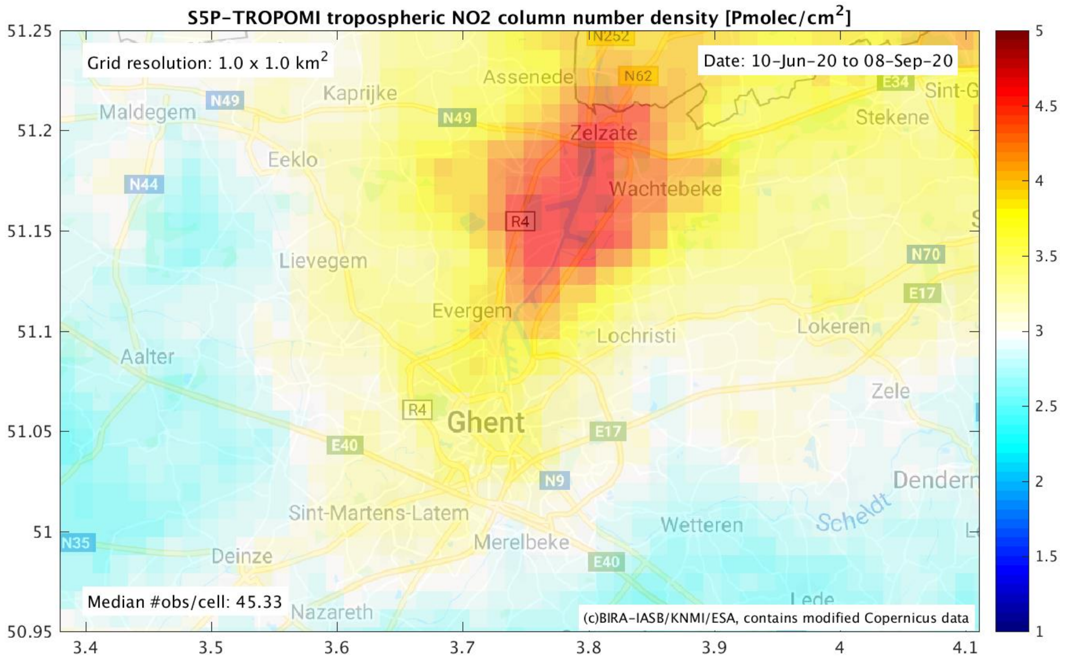

Figure 10: Map of S5p-TROPOMI tropospheric NO_2 column data over Ghent, OFFL processor versions v1.3.x, filtered on qa_value>0.75, and gridded to a 1x1km^2 resolution using data from June to August 2020.

As for the case of Antwerp (Section 5.2), Ghent (Figure 10) experiences elevated levels of NO_2 not above the city centre, but above the harbour and along the canal Ghent-Terneuzen which is a heavily industrialized region, including for instance a large site of the Arcelormittal steelworks company and a power plant (Centrale Rodenhuize) driven either with wood pellets or by waste gases from the Arcelormittal site (gases which are otherwise burned on site). Peak levels in summer 2020 (of the order of 5 Pmolec/cm^2) remain well below those observed above the harbour of Antwerp (up to 8 Pmolec/cm^2 in the 3-month average).

5.6. Liège

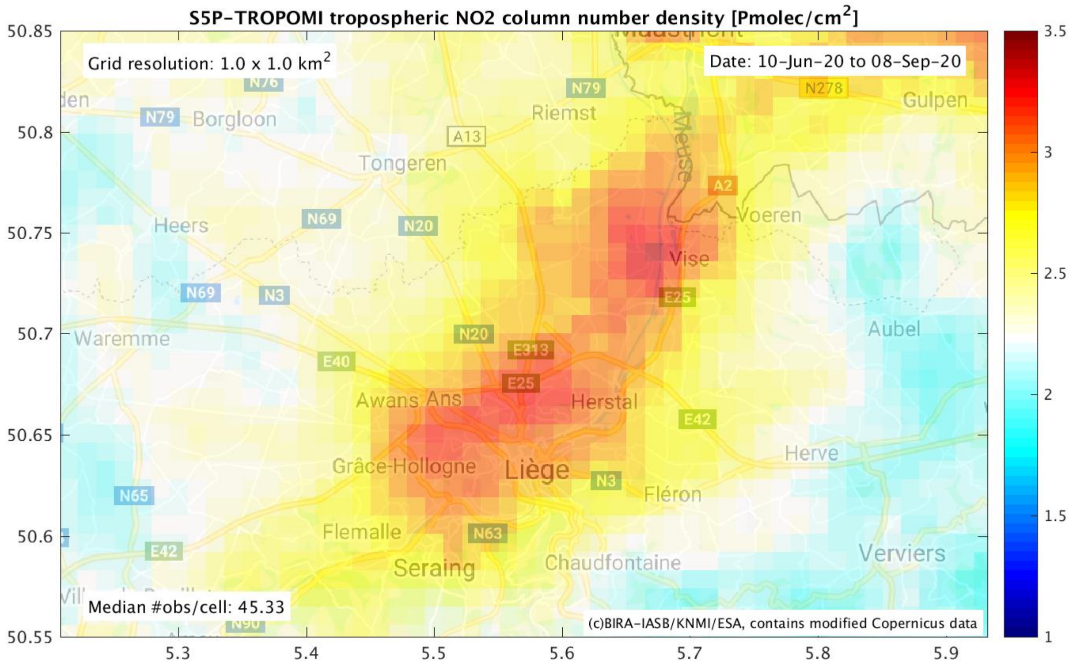

Figure 11: Map of S5p-TROPOMI tropospheric NO_2 column data over Liège, OFFL processor versions v1.3.x, filtered on qa_value>0.75, and gridded to a 1x1km^2 resolution using data from June to August 2020.

In Figure 11, we show the gridded tropospheric NO2 columns above Liège and its surroundings. The city itself is a moderate hot spot (up to 3.5 Pmolec/cm2), although there is a part in the centre that experiences slightly lower columns. A separate hot spot is evident in the North-East, just to the West of Visé. This area is mostly rural, though there is a landfill and waste management site at Hallembaye and a cement factory (CBR Lixhe).

6. Catalogue description and file access

The high-resolution maps produced hitherto are available in two formats:

- As netCDF (network Common Data Form) data files (.nc extension) for a single region covering Belgium and parts of its neighbouring countries, and for a single temporal average.
- As PNG (portable network graphics) graphics files (.png extension) for selected regions of interest, including a street map background and some essential annotations (i.e. the format of the graphics shown in the previous section)

The netCDF files

The region covered by the netCDF files is essentially that of the overpass files on which the gridding is performed (see Sect. 2 and Figure 1). The only temporal averaging windows offered to the public at this moment is 3 months (91 days), which we consider the optimum to allow the assessment of seasonal and long-term changes at increased spatial resolution.

Files are named according to the following scheme:

S5p_L3_<*area*>_<*startdate*>_<*enddate*>_<*uv*>maxWind_<*resolution*>km.nc

where <*area*> is for instance "legobox" for the entire processed area, <*startdate*> and <*enddate*> are formatted *yyyymmdd*, <*uv*> is the maximum wind speed filter in m s^{-1} (999 if not applied), and <*resolution*> the grid cell size. The netCDF file used to produce the maps in Sect. 5 is named:

S5p_L3_legobox_20200601_20200830_999maxWind_1.0km.nc

Note that the end date is not 31 August as we chose to have a fixed temporal aggregation window of 91 days for the 3-monthly averages.

The netCDF files currently contain the following variables:

- double **tropospheric_NO2_column_number_density** {time = 1, latitude = 555, longitude = 1049} [Pmolec cm-2]
- double **cloud_fraction** {time = 1, latitude = 555, longitude = 1049} [] (weighted average per grid cell, as for the tropospheric_NO2_column_number_density)
- double **datetime** {time = 1} [days since 2000-01-01] (weighted average per grid cell, as for the tropospheric_NO2_column_number_density, akin to an "effective" time)
- int32 **count** {time = 1} (total number of independent measurements contributing to the complete map)
- float **weight** {time = 1, latitude = 555, longitude = 1049} (total weight of the contributing L2 measurements, per grid cell)
- double **latitude_bounds** {latitude = 555, 2} [degree_north]
- double **longitude_bounds** {longitude = 1049, 2} [degree_east]

The PNG files

Graphics files in PNG format are produced from the netCDF files described above for the following fields-of-view (FOV): the entire overpass box (legobox), Belgium, Antwerp, Brussels, Ghent, Liege, and Mons. As the best colour scale depends heavily on the concentrations but some homogeneity is still desirable to aid intercomparisons, the maps are produced for 3 fixed colour scales: "low" (1-3.5 Pmolec/cm^2), "medium" (1-5 Pmolec/cm^2), and "high" (1-8 Pmolec/cm^2). They are organized in the following folder structure:

/<tempAvgWindow>/<colourScale>/<FOV>/

Data access

The first version of the catalogue is available through anonymous ftp at

ftp://ftp-ae.oma.be/pub/from_Tijl.Verhoelst/LEGO-BEL-AQ/Maps/

This repository will be elaborated further to cover a range in dates, temporal averaging window sizes, and filter criteria. A dedicated project ftp site will also be established, to which we can provide a direct link from the project homepage at https://lego-bel-aq.aeronomie.be.

7. Conclusions and prospects

The first set of maps presented here provides a first indication of the potential gains in resolution to be obtained by temporal aggregation and spatial oversampling of S5P-TROPOMI tropospheric NO_2 columns. This gain in resolution is found to be valuable to characterize the spatial distribution of persistently high columns of NO_2 over Belgium, allowing the differentiation between neighbouring regions of large population density (e.g. Brussels vs. the communes just North of the ring road) or city centres versus suburban industrial areas e.g. (Antwerp and Ghent vs. their harbours). While the maps and corresponding data files made available at the moment are still limited in scope, an update of the current deliverable scheduled for end of 2021 will contain further refinements and extensions in terms of aggregation criteria (other temporal windows, aggregation by weekday vs. weekend,…) and improvements in the oversampling approach using geostatistical techniques, in particular to address poor data density when averaging over smaller temporal windows. An update will also be performed when the source data (the L2 NO_2 data) are reprocessed with the latest L2 processor. This is important to be able to do a meaningful analysis of the temporal evolution (over multiple years) of the high-resolution maps, which now risks artefacts due to differential biases between processor versions (in particular the change to v1.4.0 with its updated cloud retrieval). Further work (to be reported on in other deliverables) will target the relation between the tropospheric columns mapped here and the surface concentrations as measured by in-situ instruments (and extrapolated into continuous fields using model calculations).

References

Boersma, K. F., Eskes, H. J., Veefkind, J. P., Brinksma, E. J., van der A, R. J., Sneep, M., van den Oord, G. H. J., Levelt, P. F., Stammes, P., Gleason, J. F., and et al.: Near-real time retrieval of tropospheric NO2 from OMI, Atmos. Chem. Phys., 7, 2103–2118,https://doi.org/10.5194/acp-7-2103-2007, 2007.

Boersma, K. F., Eskes, H. J., Dirksen, R. J., van der A, R. J., Veefkind, J. P., Stammes, P., Huijnen, V., Kleipool, Q. L., Sneep, M., Claas, J., Leitão, J., Richter, A., Zhou, Y., and Brunner, D.: An improved tropospheric NO2 column retrieval algorithm for the Ozone Monitoring Instrument, Atmos. Meas. Tech., 4, 1905–1928, https://doi.org/10.5194/amt-4-1905-2011, 2011.

Boersma, K. F., Eskes, H. J., Richter, A., De Smedt, I., Lorente, A., Beirle, S., van Geffen, J. H. G. M., Zara, M., Peters, E., Van Roozendael, M., Wagner, T., Maasakkers, J. D., van der A, R. J., Nightingale, J., De Rudder, A., Irie, H., Pinardi, G., Lambert, J.-C., and Compernolle, S. C.: Improving algorithms and uncertainty estimates for satellite NO2 retrievals: results from the quality assurance for the essential climate variables (QA4ECV) project, Atmospheric Measurement Techniques, 11, 6651–6678, https://doi.org/10.5194/amt-11-6651-2018, https://www.atmos-meas-tech.net/11/6651/2018/, 2018.

Dimitropoulou, E., Hendrick, F., Pinardi, G., Friedrich, M. M., Merlaud, A., Tack, F., De Longueville, H., Fayt, C., Hermans, C., Laffineur, Q., Fierens, F., and Van Roozendael, M.: Validation of TROPOMI tropospheric NO2 columns using dual-scan multi-axis differential optical absorption spectroscopy (MAX-DOAS) measurements in Uccle, Brussels, Atmos. Meas. Tech., 13, 5165–5191, https://doi.org/10.5194/amt-13-5165-2020, 2020.

Eskes, H. J. and Eichmann K.-U.: S5P MPC Product Readme Nitrogen Dioxide, Report S5P-MPC-KNMI-PRF-NO2, version 1.4, 6 August 2019, ESA, available at: http://www.tropomi.eu/documents/prf/, 17 March 2020.

Eskes, H. J, van Geffen, J. H. G. M., Boersma, K. F., Eichmann K.-U.. Apituley, A., Pedergnana, M., Sneep, M., Veefkind, J. P., and Loyola, D.: S5P/TROPOMI Level-2 Product User Manual Nitrogen Dioxide, Report S5P-KNMI-L2-0021-MA, version 3.0.0, 27 March 2019, ESA, available at: http://www.tropomi.eu/documents/pum/, last access: 17 March 2020.

van Geffen, J., Boersma, K. F., Eskes, H., Sneep, M., ter Linden, M., Zara, M., and Veefkind, J. P.: S5P TROPOMI NO2 slant column retrieval: method, stability, uncertainties and comparisons with OMI, Atmos. Meas. Tech., 13, 1315–1335, https://doi.org/10.5194/amt-13-1315-2020, 2020.

Verhoelst, T., Compernolle, S., Pinardi, G., Lambert, J.-C., Eskes, H. J., Eichmann, K.-U., Fjæraa, A. M., Granville, J., Niemeijer, S., Cede, A., Tiefengraber, M., Hendrick, F., Pazmiño, A., Bais, A., Bazureau, A., Boersma, K. F., Bognar, K., Dehn, A., Donner, S., Elokhov, A., Gebetsberger, M., Goutail, F., Grutter de la Mora, M., Gruzdev, A., Gratsea, M., Hansen, G. H., Irie, H., Jepsen, N., Kanaya, Y., Karagkiozidis, D., Kivi, R., Kreher, K., Levelt, P. F., Liu, C., Müller, M., Navarro Comas, M., Piters, A. J. M., Pommereau, J.-P., Portafaix, T., Prados-Roman, C., Puentedura, O., Querel, R., Remmers, J., Richter, A., Rimmer, J., Rivera Cárdenas, C., Saavedra de Miguel, L., Sinyakov, V. P., Stremme, W., Strong, K., Van Roozendael, M., Veefkind, J. P., Wagner, T., Wittrock, F., Yela González, M., and Zehner, C.: Ground-based validation of the Copernicus Sentinel-5P TROPOMI NO2 measurements with the NDACC ZSL-DOAS, MAX-DOAS and Pandonia global networks, Atmos. Meas. Tech., 14, 481–510, https://doi.org/10.5194/amt-14-481-2021, 2021.

Acronyms

AQ	Air Quality
AMF	Air Mass Factor or optical enhancement factor
CEOS	Committee on Earth Observations Satellites
COVID	Corona Virus Disease
CTM	Chemical Transport Model
DOAS	Differential Optical Absorption Spectroscopy
DOMINO	Dutch OMI NO2 product
ECMWF	European Centre for Medium-Range Weather Forecasts
ECV	Essential Climate Variable
ERA-5	ECMWF Reanalysis 5
FRESCO	Fast Retrieval Scheme for Clouds from the Oxygen A band
GEO	Geostationary Orbit
HARP	*Not an acronym; atmospheric data processing toolbox*
LEGO-BEL-AQ	Low-Earth and Geostationary Observations of BELgian Air Quality
LEO	Low-Earth Orbit
MAX-DOAS	Multi-Axis Differential Optical Absorption Spectroscopy
MPC	Mission Performance Centre
netCDF	Network Common Data Form
NRTI	Near Real Time
OFFL	Offline
OMI	Ozone Monitoring Instrument
PRF	Product Readme File
PSF	Point Spread Function
QA4ECV	Quality Assurance for Essential Climate Variables
S4	Sentinel 4
S5	Sentinel 5
S5P	Sentinel-5 Precursor
SZA	Solar Zenith Angle
TEMIS	Tropospheric Emission Monitoring Internet Service
TROPOMI	Tropospheric Monitoring Instrument
VDAF	Validation Data Analysis Facility